SUPPORTING INFORMATION FOR:

Supekar, S. D., D. J. Graziano, S. J. Skerlos, and J. Cresko (2020). Comparing energy and water use of aqueous and gas-based metalworking fluids. *Journal of Industrial Ecology*.

Summary

This supporting information provides (1) descriptions and relevant details for aqueous and gas-based metalworking fluids (MWFs) on which energy and water use calculations in the paper are based; (2) details of data extraction procedures used to obtain tool life, material removal rate, and MWF parameters from the published literature; and (3) supplementary results for different uncertainty scenarios and a public URL to raw data files used to create figures in the paper, as well as Ecospold and Excel® files for key MWF materials and unit processes.

Table of Contents

S1 DESCRIPTION AND DETAILS OF METALWORKING FLUIDS

S1.1 Aqueous metalworking fluid

Aqueous metalworking fluid (MWF) are typically formulated as emulsions of petroleum-based lubricants in water using several additive for MWF performance, emulsion stability, and process control (emulsifier, biocide, corrosion inhibitor, pH buffer, coupler, and extreme pressure lubricant). Delivery pressures for conventional delivery of aqueous MWF typically range from 0.5 – 3 MPa and up to 30 MPa for high-pressure delivery. Aqueous MWFs are periodically recycled in a batch process filtration process, and ultimately disposed.

S1.2 Aqueous MWF compositions

Table S1 | Composition of semi-synthetic and synthetic aqueous MWF concentrates based on (Byers 2017). Energy and water use data for MWF components obtained from (Ecoinvent 2018).

Component	Fraction (w/w)	Description	Data source and notes
Semi-synthetic concentrate			
Mineral oil	15%	Napthenic oil	Ecoinvent 3.5 material/substitute used: Lubricating oil
Anionic emulsifier	5%	Sulfonate base such as sodium petroleum sulfonate	Ecoinvent 3.5 material/substitute used: Alkylbenzene sulfonate detergent
Nonionic emulsifier	15%	Alkanolamide	Ecoinvent 3.5 material/substitute used: Diethanolamine
Biocide	2%	Triazine/Pyridiethione	Ecoinvent 3.5 material/substitute used: Triazine compound
Corrosion inhibitor	6%	Amine borate	Ecoinvent 3.5 material/substitute used: 1:1 mix of boric acid and monoethanolamine
Coupler	1.5%	Butyl carbitol	Ecoinvent 3.5 material/substitute used: Ethyleneglycol diethyl ether
Water	55.5%	Dilutant	Ecoinvent 3.5 material/substitute used: Tap water
Synthetic concentrate			
EP lubricant	4%	Phosphate ester	Ecoinvent 3.5 material/substitute used: Sodium pyrophosphate (also a plasticizer)
Boundary lubricant	9%	PEG ester	Ecoinvent 3.5 material/substitute used: Ethoxylated alcohol AE7
pH buffer	5%	Triethanolamine	Ecoinvent 3.5 material/substitute used: Triethanolamine
Biocide	2%	Triazine/Pyridiethione	Ecoinvent 3.5 material/substitute used: Triazine compound

Corrosion inhibitor	1%	Amine borate	Ecoinvent 3.5 material/substitute used: 1:1 mix of boric acid and monoethanolamine
Water	70%	Dilutant	Ecoinvent 3.5 material/substitute used: Tap water

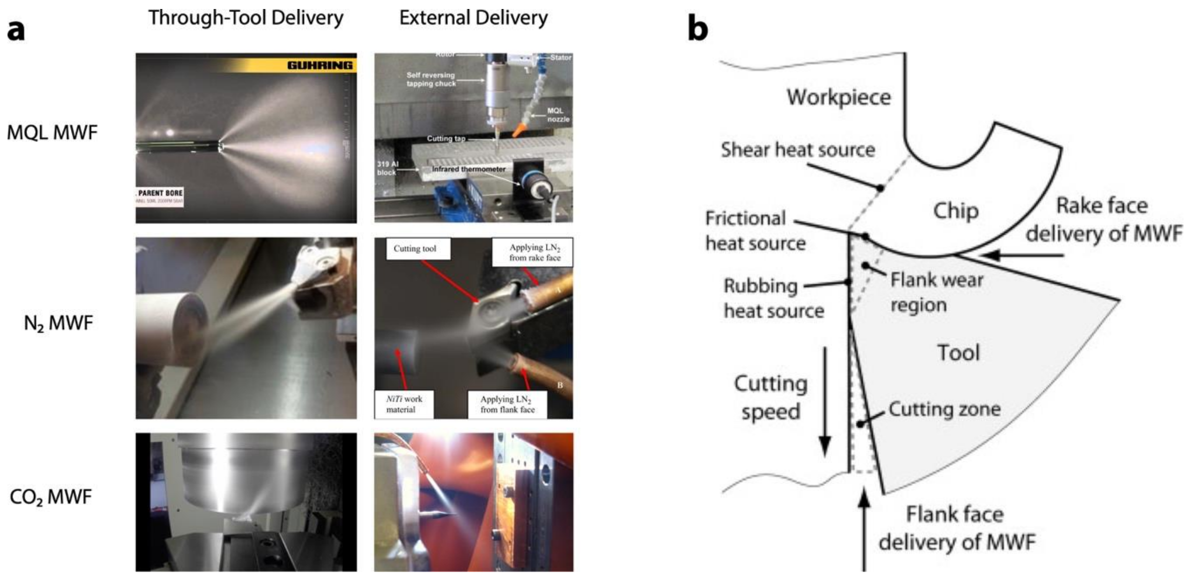

Figure S1 | **a.** External and through-tool delivery of gas-based MWFs. (Sources: top-left – (Gühring 2014); top-right (Bhowmick et al. 2010) with permission from Elsevier; mid-left (Kaynak and Gharibi 2018); mid-right – (Kaynak et al. 2013) with permission from Elsevier; bottom-left – (Fusion Coolant Systems Inc. 2015); bottom-right – (Supekar et al. 2013) with permission from ASME. **b.** Cutting tool-workpiece interface and sources of heat generation in machining. Source: (Wang and Clarens 2013) with permission from Elsevier.

All three gas-based MWFs described next can be delivered through the cutting tool or through external nozzles as shown in Figure S1a. Unlike water, gas-based MWFs do not exhibit surface tension and are therefore able to penetrate deeper into the geometry of the cutting tool-workpiece interface, and provide more effective cooling and lubrication to the regions where frictional and shearing-based heat generation predominantly occur as shown in Figure S1b.

S1.3 Oil-in-air minimum quantity lubrication metalworking fluid

MQL: Minimum quantity lubrication MWF is a spray of atomized particles of lubricant, typically a plant-derived oil, delivered in compressed air. Compressed air pressures typically range between 0.4 – 0.7 MPa, and lubricant consumption rates are of the order of tens of milliliters per hour.

S1.4 Carbon dioxide-based metalworking fluid

CO_2 MWF is a spray of rapidly expanding liquid or supercritical CO_2 through a nozzle. CO_2 MWF typically contains dissolved or over-saturated mineral or vegetable oil lubricant with oil consumption rates ranging from tens to hundreds of milliliters per hour. Rapid expansion from liquid or supercritical state creates a stream of chilled CO_2 gas cold and dry ice particles at about

–80 °C. When a lubricant is used with CO_2 MWF, the chilled oil particles provide nuclei for precipitation of the dry ice particles (Tom and Debenedetti 1991).

S1.5 Nitrogen-based metalworking fluid

N_2 MWF is a spray of compressed gaseous or liquid N_2 delivered through a nozzle with or without a lubricant. N_2 experiences rapid expansion through the nozzle and spray temperatures are typically about –195 °C.

S1.6 MWF delivery energy calculations

Electric power for pumping aqueous is obtained using equation (S1). Electric power for compressing gas-based before delivery (air and CO_2) is calculated using equation (S2). Here, MWF mass flow rate ($\dot{m}$, kg/min) and final delivery pressure (p_2, MPa) are obtained from individual experimental studies examined, and other parameters such as density (ρ), adiabatic coefficient (γ), and efficiencies needed to calculate delivery power are applied based on values provided in Table S2. For aqueous MWF, the density of emulsion is assumed to be equal to density of water since oil concentrations are small (< 5% w/w).

$$P_{aqueous}^{delivery}\left\{\tfrac{MJ}{min}\right\} = \dot{m}_{water}\left\{\tfrac{kg}{min}\right\}\left(\frac{p_2 - p_1\{MPa\}}{\rho_{water}\eta_{mechanical}}\right) \tag{S1}$$

$$P_{gas}^{delivery}\left\{\tfrac{MJ}{min}\right\} = \frac{\dot{m}_{gas}\left\{\tfrac{kg}{min}\right\}\left(\dfrac{p_1\{MPa\}\gamma}{\gamma - 1}\right)\left(\left(\dfrac{p_2}{p_1}\right)^{\frac{\gamma-1}{\gamma}} - 1\right)}{\rho_{gas}\left\{\tfrac{kg}{m^3}\right\}\eta_{adiabatic}\eta_{mechanical}} \tag{S2}$$

Table S2 | Metalworking fluid parameters used to calculate MWF delivery power consumption. This power is multiplied with the annual "up" time calculated in equation (1) to obtain MWF delivery energy use.

	Density (ρ, kg/m^3)	**Mechanical efficiency ($\eta_{mechanical}$)**	**Adiabatic efficiency ($\eta_{adiabatic}$)**	**C_p/C_v (γ)**	**Initial pressure (p_1, MPa)**
Water	1000	60%	-	-	0.1
Supercritical CO_2	798	87%	82%	2.7450	2
Liquid CO_2	736	87%	82%	7.9292	2
Gaseous CO_2	132	87%	82%	2.2445	2
Air	8.2	87%	82%	1.3935	0.1

S1.7 Aqueous MWF recycling and disposal energy calculations

S1.7.1 Recycling

The aqueous MWF recycling process assumes batch filtration of the contents of the 378 L (100 gallon) sump at a specified frequency each month (see Table 2). The process involves (1) draining the sump using a pump (assumed at 0.4 MPa and 20 gallons per minute flow rate) for 2 minutes;

(2) pasteurization to 74 °C (Byers 2017) from an initial temperature of 25 °C; (3) microfiltration at a pressure of 0.7 MPa and 1.5 gallons per minute flow rate for 67 minutes; and (4) discharging filtered MWF back into the sump at 0.15 MPa and 1.5 gallons per minutes for 67 minutes (Wendt 2018; Eriez 2012). Pumping power consumption is calculated using equation (S1), and total pumping energy consumption is calculated by multiplying pumping power in each step with its respective process time specified above. Pasteurization energy use is calculated as the product of the total mass of the water (378 kg), the specific heat of the MWF (assumed equal to that of water, 4.2 kJ/kg°C), and the temperature increase (74 – 25 = 49 °C). Efficiency of electrical input to pasteurization heat is assumed at 90%.

S1.7.2 Disposal

Disposal methods for aqueous MWF range include a primary treatment process to separate free oils and solids from the emulsion, a secondary treatment process, and frequently, a tertiary treatment process to prepare the wastewater for discharge to natural water bodies or to public wastewater treatment facilities. A detailed description on the wide range of MWF waste disposal methods found in practice can be found in (Byers 2017).

The treatment chain modeled in this work assumes the primary treatment as separation in a settling tank, from which energy and water impacts are considered negligible. The secondary and tertiary treatment were chosen as ultrafiltration (UF) and nanofiltration (NF), respectively, since such a system is able to handle both semi-synthetic and synthetic used MWF wastewater and the technologies used are commercially mature, well-characterized, and relatively inexpensive in terms of capital costs. Following the filtration steps, the concentrated oil waste is sent for hazardous waste incineration and the wastewater is sent for treatment to a small-sized (1 million m^3/year capacity) municipal wastewater treatment works. All life cycle inventory data for materials/processes considered in the disposal process are from Ecoinvent 3.5 global averages unless US-specific data were available.

The filters for both UF and NF processes, we assumed the filter cartridge to be comprised of 18 cylindrical tubes of 0.0125 m in diameter and 1 m in length, providing a collective membrane surface area of about 0.7 m^2 (Hilal et al. 2004). For UF, a membrane pressure of 4 bar was assumed, at which a permeate flow rate of 39 L/m^2/hour was reported by (Hilal et al. 2004). Based on the calculated membrane surface area, filtering each batch of 100 gallon (378 L) would require 13.7 hours. Further, based on (Byers 2017), for each L/min of permeate flow, 50 L/min of cross flow of the MWF is typically needed. Using equation (S1), the pumping power needed for this process is calculated to be about 15.7 kW assuming a mechanical efficiency of 58.5% (90% electrical motor efficiency x 65% pump efficiency). The UF electricity requirement per batch is then calculated as the product of this pumping power and filtration time – about 775 MJ/batch.

Similarly, NF filtration pressure and corresponding permeate flow was assumed to be 7 bar and 22 L/m^2/hour based on (Hilal et al. 2004). The filtration time per 100 gallon batch is calculated to be about 24.3 hours, and the pumping power is calculated equation (S1) as 15.5 kW assuming the same ratio of permeate flow to cross-flow as UF. The NF electricity use is thus calculated as 1360 MJ/batch. It is assumed that at the end of the UF + NF process, all emulsified oil at 5% w/w concentration in the sump is fully recovered and sent for hazardous waste incineration using a long haul 7 – 16 tonne capacity long haul truck. The remaining 95% w/w of the wastewater is sent for municipal wastewater treatment.

S2 DATA EXTRACTION FROM PUBLISHED STUDIES

The studies shown in Table S3 met the screening criteria described in section 2.3 of the main body of the paper. The specific MWF comparison and number of experiments used in the analysis in this paper is also indicated in Table S3.

Table S3 | List of experimental studies from the literature used to evaluate and compare the contributions of aqueous and gas-based MWFs to the embodied energy and water of machined materials. † indicates that aqueous MWF was applied as a high-pressure coolant.

Study	**Aqueous v. CO_2**	**Aqueous v. MQL**	**Aqueous v. N_2**	**Number of unique experiments**
(Aramcharoen 2016)			✓	1
(Bermingham et al. 2012)†			✓	2
(Braga et al. 2002)		✓		2
(Braghini Junior et al. 2009)		✓		1
(Da Silva et al. 2011)		✓		4
(Dhar and Kamruzzaman 2007)			✓	1
(Dhar et al. 2006)		✓		1
(Garcia and Ribeiro 2016)		✓		3
(Hong et al. 2001)			✓	3
(Khan and Ahmed 2008)			✓	16
(Khan et al. 2009)		✓		1
(Kirsch et al. 2018)	✓		✓	2
(Liao et al. 2007)		✓		9
(López de Lacalle et al. 2006)		✓		2
(Machai and Biermann 2011)	✓			3
(MacLean et al. 2009)	✓			2
(Mulyadi et al. 2015)		✓		1
(Obikawa et al. 2008)		✓		1
(Paul et al. 2001)			✓	1
(Priarone et al. 2012)		✓		5
(Pušavec and Kopač 2011)			✓	1
(Sadik et al. 2016)†	✓			3
(Sreejith 2008)		✓		1
(Stanford et al. 2009)			✓	1
(Stephenson et al. 2014)	✓			1

(Sun et al. 2006)		✓		5
(Supekar et al. 2012)	✓	✓	✓	5
(Wika et al. 2019)	✓			4
(Yan et al. 2012)		✓		4

The *MRR* in cm^3/min for turning, milling, and drilling processes is calculated using equations (S3) – (S5), respectively. Here, v (m/min) is the cutting speed, a_p (mm) is the axial depth of cut in turning and milling, a_e (mm) is the radial depth of cut in milling, f (mm/rev) is the feed rate, and D (mm) is the diameter of the milling cutter or drill. For multi-tooth milling cutters and multi-fluted drills, the feed f is calculated as the product of the feed per tooth or flute, f_z, and the number of teeth or flutes, Z. Values for each of these parameters are obtained from individual studies. Tool life (T_{mc}) is similarly either obtained directly from reported values in a study, or extracted from tool wear progression curves as shown in Figure S2.

$$MRR_{turning} = a_p f v \quad \text{(S3)}$$

$$MRR_{milling} = \frac{a_p a_e f v}{\pi D} \quad \text{(S4)}$$

$$MRR_{drilling} = \frac{D f v}{4} \quad \text{(S5)}$$

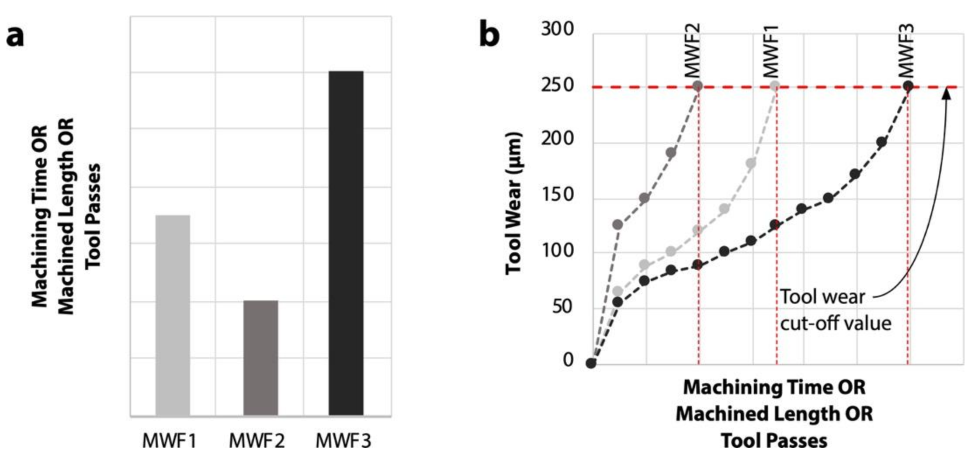

Figure S2 | Tool life used to obtain throughput using equation (1) is obtained from **a.** directly reported values or from **b.** tool wear progression charts.

The MWF flow rate, pressure, and lubricant concentration reported within each experiment are used to calculate the annual energy and water use associated with the consumptive use and delivery of the MWF according to the scope shown in Figure 1a. Embodied energy is then calculated using the process depicted in Figure S3. We note that when experiments for a unique material-process-machining conditions combination are replicated in a study, we use the mean value of the replicates to calculate the embodied energy and water of material machined.

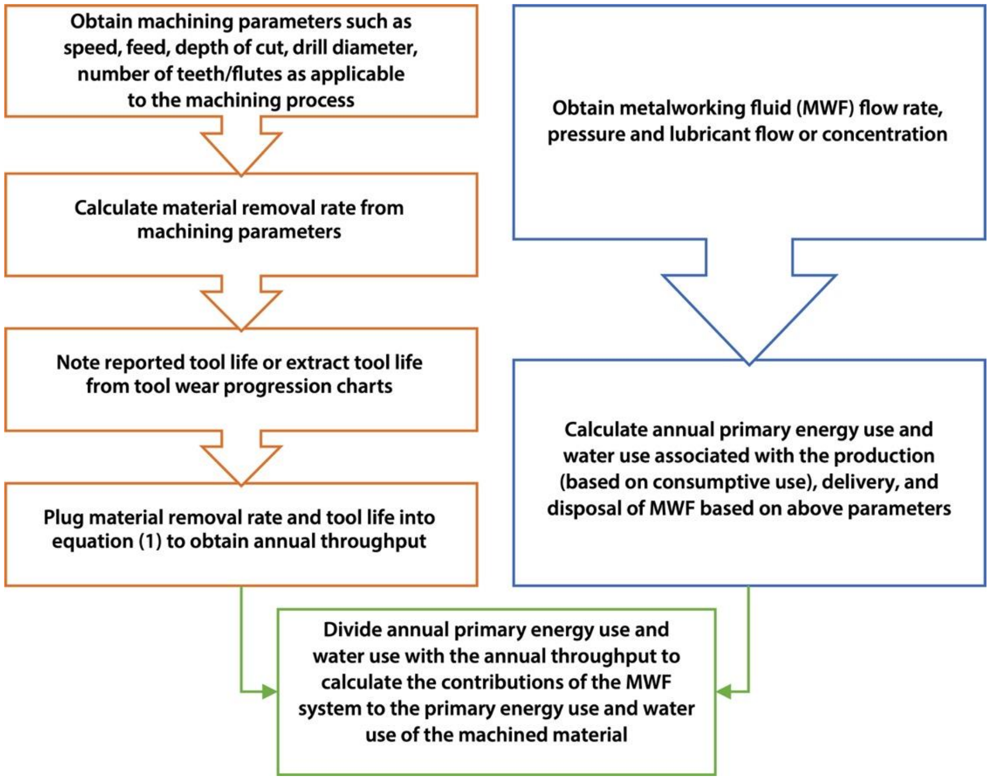

126

127 Figure S3 | Flow chart showing the process of calculating primary energy use and water use per unit of
128 material machined for each paired experimental comparison of MWFs in the studies listed in Table S3 from
129 their reported machining and MWF operational parameters.

130 S3 SUPPLEMENTARY RESULTS

131 S3.1 Embodied primary energy and water in aqueous and gas-based MWF components

132 Table S4 | Embodied primary energy and water in each component of aqueous and gas-based MWFs.

MWF Component	Embodied Primary Energy (MJ/unit)	Embodied Water Depletion (L/unit)
Tap water (unit = 1 kg)	3.55E-03	1.05E+00
Semi-synthetic mineral oil concentrate[a] (unit = 1 kg)	3.17E+01	3.47E+00
Synthetic mineral oil concentrate[a] (unit = 1 kg)	1.97E+01	3.65E+00
Vegetable oil (unit = 1 kg)	9.62E+01	2.43E+02
CO_2 ≥ 99.9% purity[b] (unit = 1 kg)	5.75E+00	7.74E-01
N_2 ≥ 99.95% purity[b] (unit = 1 kg)	9.73E+00	2.07E+00

[a]Includes commonly used additives described in Table S1; [b]Transportation accounted for separately

133

S3.2 Results for the other scenarios

S3.2.1 Best-worst scenario

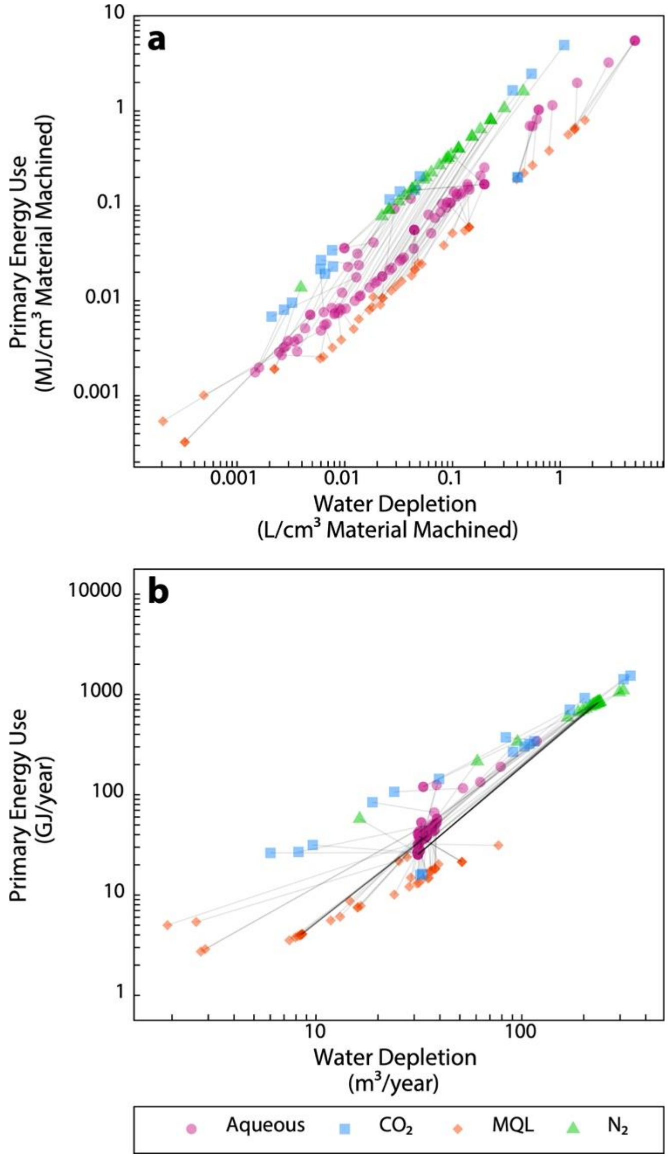

Figure S4 | Primary energy use and water use associated with the production, delivery, and disposal of MWFs expressed **a.** per unit volume of material machined over a year, and **b.** on an annual basis for the best-case parameters for gas-based MWFs compared against worst-case parameters for aqueous MWF. Underlying data used to create this figure can be found in the data repository (Supekar et al. 2019) using this link.

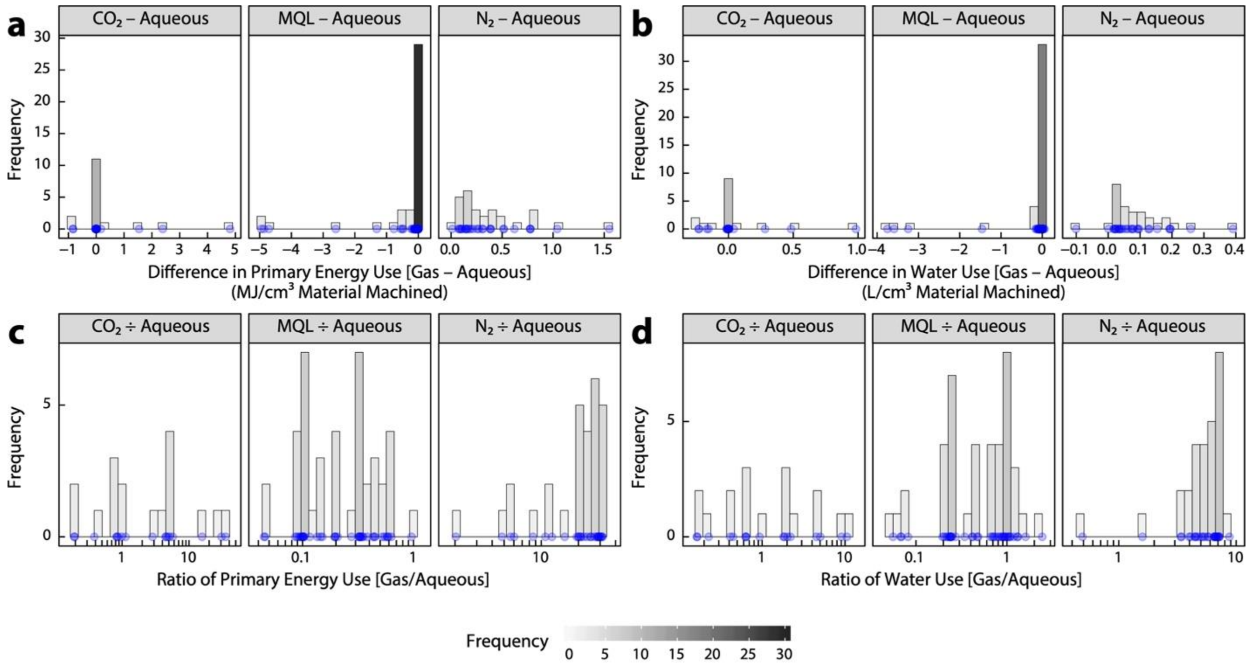

Figure S5 | Differences in **a.** primary energy use and **b.** water use per unit of material machined using gas-based and aqueous MWFs based on reported MWF conditions and machining parameters in the experimental literature for the best-case parameters for gas-based MWFs compared against worst-case parameters for aqueous MWF. Ratios of **c.** primary energy use and **d.** water use corresponding to the differences in paired data shown in a–b, where a ratio of 1 indicates that the primary energy or water use for the gas-based MWF is equal to that of the aqueous MWF in a given paired experiment. Blue dots represent the differences and ratios in primary energy and water use in individual experiments on which the histograms in the figure are based. Underlying data used to create this figure can be found in the data repository (Supekar et al. 2019) using this link.

S3.2.2 Worst-best scenario

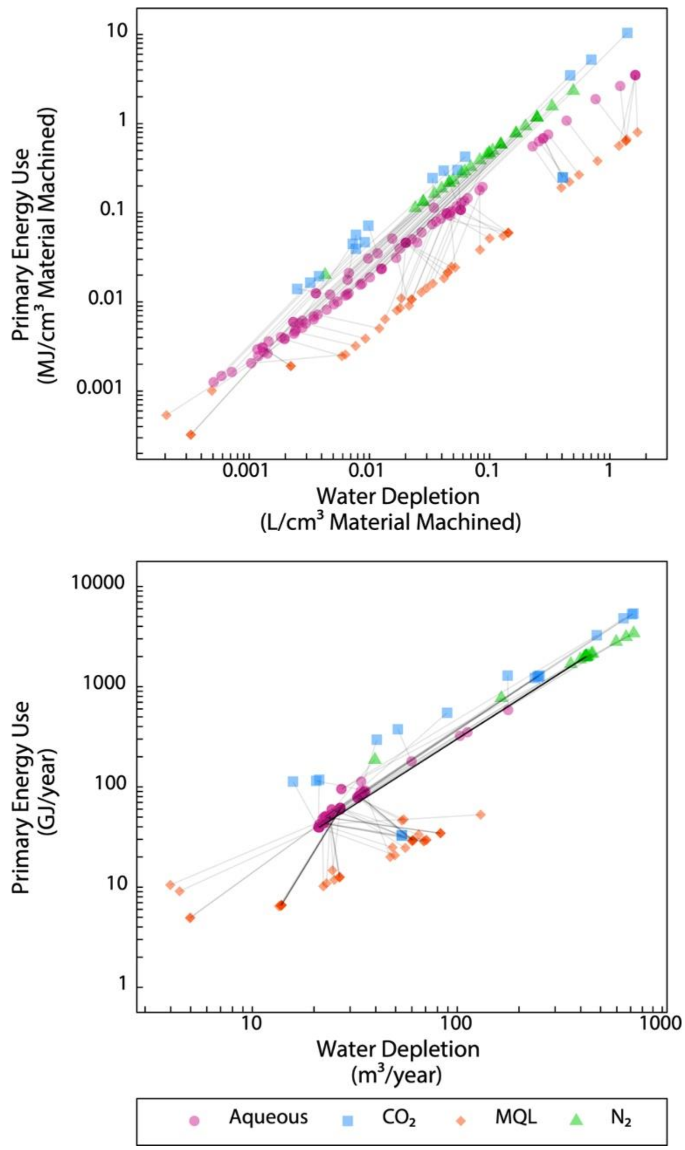

Figure S6 | Primary energy use and water use associated with the production, delivery, and disposal of MWFs expressed **a.** per unit volume of material machined over a year, and **b.** on an annual basis for the worst-case parameters for gas-based MWFs compared against best-case parameters for aqueous MWF. Underlying data used to create this figure can be found in the data repository (Supekar et al. 2019) using this link.

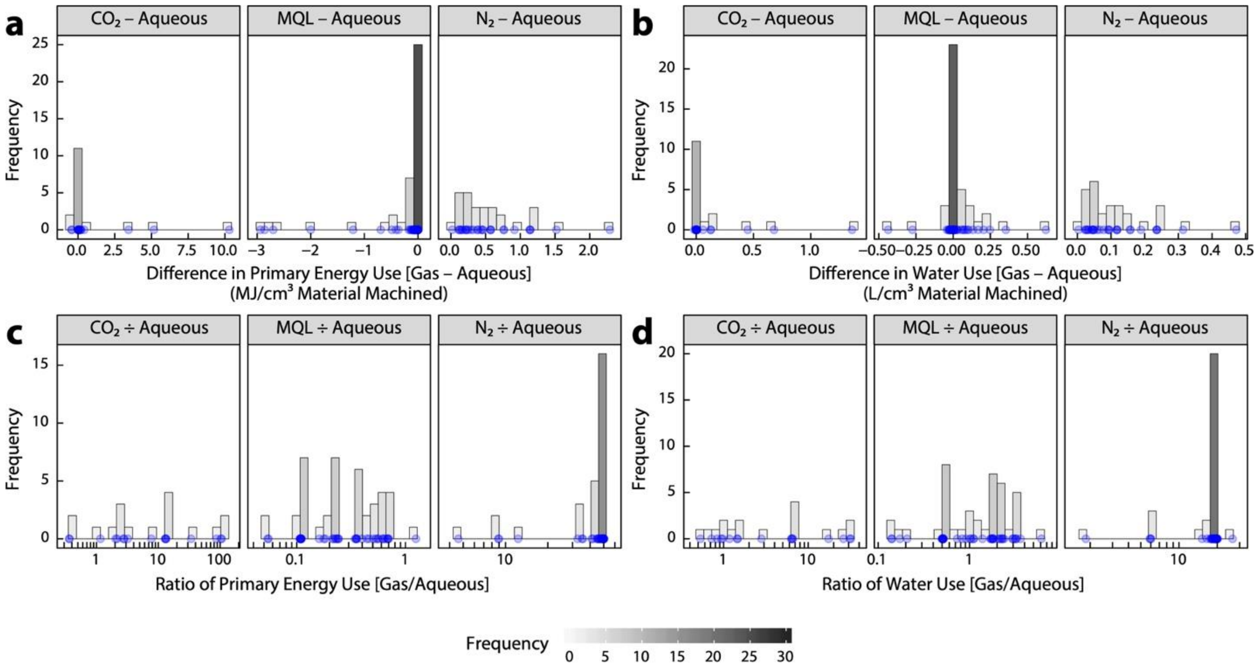

Figure S7 | Differences in **a.** primary energy use and **b.** water use per unit of material machined using gas-based and aqueous MWFs based on reported MWF conditions and machining parameters in the experimental literature for the worst-case parameters for gas-based MWFs compared against best-case parameters for aqueous MWF. Ratios of **c.** primary energy use and **d.** water use corresponding to the differences in paired data shown in a–b, where a ratio of 1 indicates that the primary energy or water use for the gas-based MWF is equal to that of the aqueous MWF in a given paired experiment. Blue dots represent the differences and ratios in primary energy and water use in individual experiments on which the histograms in the figure are based. Underlying data used to create this figure can be found in the data repository (Supekar et al. 2019) using this link.

S3.3 Life cycle inventory and results repository

Ecospold and Excel® files for key MWF materials and unit processes, and results datasets used to create the figures in this paper can be accessed free of charge in the data repository by (Supekar et al. 2019) using the following link – https://doi.org/10.5281/zenodo.3565781.

REFERENCES

Aramcharoen, A. 2016. Influence of Cryogenic Cooling on Tool Wear and Chip Formation in Turning of Titanium Alloy. *Procedia CIRP* 46: 83–86.

Bermingham, M.J., S. Palanisamy, D. Kent, and M.S. Dargusch. 2012. A comparison of cryogenic and high pressure emulsion cooling technologies on tool life and chip morphology in Ti–6Al–4V cutting. *Journal of Materials Processing Technology* 212(4): 752–765.

Bhowmick, S., M.J. Lukitsch, and A.T. Alpas. 2010. Tapping of Al–Si alloys with diamond-like carbon coated tools and minimum quantity lubrication. *Journal of Materials Processing Technology* 210(15): 2142–2153.

Braga, D.U., A.E. Diniz, G.W.A. Miranda, and N.L. Coppini. 2002. Using a minimum quantity of lubricant (MQL) and a diamond coated tool in the drilling of aluminum–silicon alloys. *Journal of Materials Processing Technology* 122(1): 127–138.

Braghini Junior, A., A.E. Diniz, and F.T. Filho. 2009. Tool wear and tool life in end milling of 15–5 PH stainless steel under different cooling and lubrication conditions. *The International Journal of Advanced Manufacturing Technology* 43(7–8): 756–764.

Byers, J.P. 2017. *Metalworking Fluids*. 3rd Edition. Boca Raton, FL: Taylor & Francis, September 18. https://www.taylorfrancis.com/books/e/9781498722230.

Da Silva, R.B., J.M. Vieira, R.N. Cardoso, H.C. Carvalho, E.S. Costa, A.R. Machado, and R.F. De Ávila. 2011. Tool wear analysis in milling of medium carbon steel with coated cemented carbide inserts using different machining lubrication/cooling systems. *Wear* 271(9–10): 2459–2465.

Dhar, N.R. and M. Kamruzzaman. 2007. Cutting temperature, tool wear, surface roughness and dimensional deviation in turning AISI-4037 steel under cryogenic condition. *International Journal of Machine Tools and Manufacture* 47(5): 754–759.

Dhar, N.R., M. Kamruzzaman, and M. Ahmed. 2006. Effect of minimum quantity lubrication (MQL) on tool wear and surface roughness in turning AISI-4340 steel. *Journal of Materials Processing Technology* 172(2): 299–304.

Ecoinvent. 2018. *LCI Database v3.5*. Zurich, Switzerland: ETH Zurich; EPF Lausanne; Swiss Federal Laboratories for Materials Science and Technology; Institute for Sustainability Sciences; Agroscope. https://www.ecoinvent.org/home.html.

Eriez. 2012. SumpDoc Brochure. https://www.vision-solutions.ca/media/uploads/products/files/Hydroflow_SumpDocBrochure_VB340IP.pdf.

Fusion Coolant Systems Inc. 2015. Fusion Coolant Systems. September 15. https://youtu.be/ymYLG7X9se4. Accessed May 22, 2019.

Garcia, U. and M.V. Ribeiro. 2016. Ti6Al4V Titanium Alloy End Milling with Minimum Quantity of Fluid Technique Use. *Materials and Manufacturing Processes* 31(7): 905–918.

Gühring. 2014. MQL - GÜHRING. July 18. https://youtu.be/0D5sUnS0q0Q. Accessed May 5, 2019.

Hilal, N., G. Busca, N. Hankins, and A.W. Mohammad. 2004. The use of ultrafiltration and nanofiltration membranes in the treatment of metal-working fluids. *Desalination* 167: 227–238.

Hong, S.Y., I. Markus, and W. Jeong. 2001. New cooling approach and tool life improvement in cryogenic machining of titanium alloy Ti-6Al-4V. *International Journal of Machine Tools and Manufacture* 41(15): 2245–2260.

Kaynak, Y. and A. Gharibi. 2018. Progressive Tool Wear in Cryogenic Machining: The Effect of Liquid Nitrogen and Carbon Dioxide. *Journal of Manufacturing and Materials Processing* 2(2): 31.

Kaynak, Y., H.E. Karaca, R.D. Noebe, and I.S. Jawahir. 2013. Tool-wear analysis in cryogenic machining of NiTi shape memory alloys: A comparison of tool-wear performance with dry and MQL machining. *Wear* 306(1–2): 51–63.

Khan, A.A. and M.I. Ahmed. 2008. Improving tool life using cryogenic cooling. *Journal of Materials Processing Technology* 196(1–3): 149–154.

Khan, M.M.A., M.A.H. Mithu, and N.R. Dhar. 2009. Effects of minimum quantity lubrication on turning AISI 9310 alloy steel using vegetable oil-based cutting fluid. *Journal of Materials Processing Technology* 209(15–16): 5573–5583.

Kirsch, B., S. Basten, H. Hasse, and J.C. Aurich. 2018. Sub-zero cooling: A novel strategy for high performance cutting. *CIRP Annals* 67(1): 95–98.

Liao, Y.S., H.M. Lin, and Y.C. Chen. 2007. Feasibility study of the minimum quantity lubrication in high-speed end milling of NAK80 hardened steel by coated carbide tool. *International Journal of Machine Tools and Manufacture* 47(11): 1667–1676.

López de Lacalle, L.N., C. Angulo, A. Lamikiz, and J.A. Sánchez. 2006. Experimental and numerical investigation of the effect of spray cutting fluids in high speed milling. *Journal of Materials Processing Technology* 172(1): 11–15.

Machai, C. and D. Biermann. 2011. Machining of β-titanium-alloy Ti–10V–2Fe–3Al under cryogenic conditions: Cooling with carbon dioxide snow. *Journal of Materials Processing Technology* 211(6): 1175–1183.

MacLean, D.J., K.F. Hayes, T. Barnard, T. Hull, Y.E. Park, and S.J. Skerlos. 2009. Impact of Supercritical Carbon Dioxide Metalworking Fluids on Tool Life in Turning of Sintered Steel and Milling of Compacted Graphite Iron. In *ASME 2009 International Manufacturing Science and Engineering Conference, Volume 1*, 43–48. West Lafayette, Indiana, USA: ASME. http://proceedings.asmedigitalcollection.asme.org/proceeding.aspx?articleid=1633203. Accessed August 17, 2018.

Mulyadi, I.H., V.A. Balogun, and P.T. Mativenga. 2015. Environmental performance evaluation of different cutting environments when milling H13 tool steel. *Journal of Cleaner Production* 108: 110–120.

Obikawa, T., Y. Kamata, Y. Asano, K. Nakayama, and A.W. Otieno. 2008. Micro-liter lubrication machining of Inconel 718. *International Journal of Machine Tools and Manufacture* 48(15): 1605–1612.

Paul, S., N.R. Dhar, and A.B. Chattopadhyay. 2001. Beneficial effects of cryogenic cooling over dry and wet machining on tool wear and surface ®nish in turning AISI 1060 steel. *Journal of Materials Processing Technology*: 5.

Priarone, P.C., S. Rizzuti, G. Rotella, and L. Settineri. 2012. Tool wear and surface quality in milling of a gamma-TiAl intermetallic. *The International Journal of Advanced Manufacturing Technology* 61(1–4): 25–33.

Pušavec, F. and J. Kopač. 2011. Sustainability Assessment: Cryogenic Machining of Inconel 718. *Strojniški Vestnik – Journal of Mechanical Engineering* 57(09): 637–647.

Sadik, M.I., S. Isakson, A. Malakizadi, and L. Nyborg. 2016. Influence of Coolant Flow Rate on Tool Life and Wear Development in Cryogenic and Wet Milling of Ti-6Al-4V. *Procedia CIRP* 46: 91–94.

Sreejith, P.S. 2008. Machining of 6061 aluminium alloy with MQL, dry and flooded lubricant conditions. *Materials Letters* 62(2): 276–278.

Stanford, M., P.M. Lister, C. Morgan, and K.A. Kibble. 2009. Investigation into the use of gaseous and liquid nitrogen as a cutting fluid when turning BS 970-80A15 (En32b) plain carbon steel using WC–Co uncoated tooling. *Journal of Materials Processing Technology* 209(2): 961–972.

Stephenson, D.A., S.J. Skerlos, A.S. King, and S.D. Supekar. 2014. Rough turning Inconel 750 with supercritical CO2-based minimum quantity lubrication. *Journal of Materials Processing Technology* 214(3): 673–680.

Sun, J., Y.S. Wong, M. Rahman, Z.G. Wang, K.S. Neo, C.H. Tan, and H. Onozuka. 2006. Effects of Coolant Supply Methods and Cutting Conditions on Tool Life in End Milling Titanium Alloy. *Machining Science and Technology* 10(3): 355–370.

Supekar, S.D., A.F. Clarens, D.A. Stephenson, and S.J. Skerlos. 2012. Performance of supercritical carbon dioxide sprays as coolants and lubricants in representative metalworking operations. *Journal of Materials Processing Technology* 212(12): 2652–2658.

Supekar, S.D., B.A. Gozen, B. Bediz, O.B. Ozdoganlar, and S.J. Skerlos. 2013. Feasibility of Supercritical Carbon Dioxide Based Metalworking Fluids in Micromilling. *Journal of Manufacturing Science and Engineering* 135(2): 024501.

Supekar, S.D., D.J. Graziano, S.J. Skerlos, and J. Cresko. 2019. LCI data for materials and processes comparing energy and water use of aqueous and gas-based metalworking fluids. Zenodo, December 6. https://doi.org/10.5281/zenodo.3565781.

Tom, J.W. and P.G. Debenedetti. 1991. Particle formation with supercritical fluids—a review. *Journal of Aerosol Science* 22(5): 555–584.

Wang, S. and A.F. Clarens. 2013. Analytical model of metalworking fluid penetration into the flank contact zone in orthogonal cutting. *Journal of Manufacturing Processes* 15(1): 41–50.

Wendt, R. 2018. Cutting fluid maintenance and disposal discussion with Sump Doc© product manager at EriezTelephone. November 14.

Wika, K.K., P. Litwa, and C. Hitchens. 2019. Impact of supercritical carbon dioxide cooling with Minimum Quantity Lubrication on tool wear and surface integrity in the milling of AISI 304L stainless steel. *Wear* 426–427: 1691–1701.

Yan, L., S. Yuan, and Q. Liu. 2012. Influence of minimum quantity lubrication parameters on tool wear and surface roughness in milling of forged steel. *Chinese Journal of Mechanical Engineering* 25(3): 419–429.